Combustion Control in a Fuel Oil Boiler from the Flame Spectrum

O. FARIAS and Ph. NGENDAKUMANA
Thermodynamics Laboratory
University of Liège - Belgium

ABSTRACT

A new concept of combustion control system, based on an optical information from the flame spectrum, is applied to a domestic fuel oil boiler. The objective is to achieve the maximum thermal efficiency of the boiler, while keeping a stable flame and the pollutant emissions as low as possible. CH radicals and soot continuum emissions, measured with a spectrometer just downstream of the burner exit, provide the information needed.

Characterisation tests of the system's dynamics in different operating conditions where made in order to optimise the controller performance and to verify the sensor response in face to external factors. For a given burner power, the control is performed by varying only the air damper position (the flame holder position was fixed). This solution led to minimal NO emission with an improved flame stability. On the other hand, the sensor follows well changes in fuel properties and ambient conditions (external disturbances).

The control strategy was tested for two power conditions (high and low firing rates of the burner). Optimal values of air excess less than 6% have been achieved for both conditions. The main limitation arise from large soot production at low firing rate where the soot emission level was found around five times greater than at high firing rate.

1. INTRODUCTION

After the energetic crisis of the 1970's, the energy conservation was the only one main objective of the combustion system designers. But, with the more and more strict legislations about emission levels [1], a reduction of pollutants emission constitutes a new challenge. As a first response to these requirements, so called "Low-NOx Burners" are put on the market [2].

Currently, combustion in domestic hot water boilers is not controlled at all. For a given load, fuel and air circuits are only preadjusted manually. After the burner is ON, one expects that the adjustment was well made and that the boiler-burner combination works with a good thermal efficiency while keeping the pollutants emission level as low as possible [3]. Although such global adjustment is easily accomplished, air-fuel ratios that one obtains may differ by 15%-20% [4] with the concomitant loss of boiler efficiency if the air excess is too high. On the other hand, the influence of external conditions on the manual preadjustment is not yet well known.

Concerning the new gas burners technologies, Levinsky [5] recall the impending necessity for meeting independent requirements for flame stability, and pollutants emission (NOx and CO);

in practice, an improvement of one of these factors often results in a deterioration in the others.
In fuel oil appliances, the interaction between an evaporating fuel spray and a reacting turbulent flowfield poses an additional problem: the soot formation. Of course, the role played by the soot chemistry is highlighted by the impact of soot on the other pollutants [6]. An example is given by the well-known trade-off between the NOx emissions and the emissions of soot particulates and CO, which limit the capabilities to meet the requirements for all regulated emissions using existing combustion modification technologies [7].

Fundamental studies on flame structure by spectral and laser-based methods [8,9] have given the base for incipient applications to combustion control by means of optical methods [4,10,11,3]. Specific emissions of free radicals (OH, CH and C_2) and soot radiation provide suitable information on the processes (pollutant formation, heat release and flame stability) which occur in the reaction zone. Table 1 summarises the main aspects of the different control approaches found in the literature and the method proposed in the present study.

Table 1: *Different approaches to Combustion Control*

Reference	**Flame type/ Application**	**Sensor / main parameters**	**Method**	**Objectives**
Allen et al. 1993, [4]	Fuel oil / Laboratory	CCD camera / CH and OH	Imaging Network	• Flame stability
Schuler et al. 1994 [10]	Waste / Industrial 40MW	IR scanner camera/ Temperature (at ≈ 3.9μm)	Thermography Assisted Comb. Control	• Reduction of CO and unburned hydrocarbons
Bowman et al,1995 [11]	Premixed C_2H_4+air / Laboratory	Photodiodes / CH and C_2	Adaptive optimal control	• Volumetric heat release (max.) • Pressure fluctuations (min.)
Present work	Fuel oil / Boiler 370 kW	Spectrometer (V & near IR)/ CH and soot	On-line optimal control	• Thermal boiler efficiency, max • CO and NOx emissions (min.) • Flame stability

2. THE FLAME SPECTRUM AND THE COMBUSTION PROCESSES

The main radicals bands of CH and C_2 (at 432 and 516 nm, respectively) exist in appreciable quantities only in the reaction zone of hydrocarbon flames [8]. In premixed flames, these radicals bands appear superposed to a CO continuum that extends from 300 to 550 nm [12,13]. In a fuel oil flame, a typical spectrum, recorded just downstream of the burner exit, shows an additional contribution due to the soot emission [3,14,15].

From these radicals, CH appears as the best tracer of the flame front [16], and it has been largely used as an indicator of the local volumetric energy release [4,11,17,18] and in the detection of combustion instabilities [4].

In a first attempt to establish relationships between combustion and flame spectrum, an investigation of the evolutions of C_2 and CH radicals emissions in different operating conditions of the boiler has been performed [15]. The results have shown a strong correlation between the C_2/CH emission intensities ratio and the richness of the fuel-air mixture that was also confirmed in internal combustion engines by Chou and Patterson [13]. The C_2/CH ratio increases continuously when the global air excess is decreased and, therefore, correlates well with the thermal boiler efficiency [15,19].

In order to find also relationships between the flame spectrum and the pollutant formation mechanisms, two new parameters have been defined: *the CH+CO relative intensity and the integrated soot radiation* [20].

Figure 1 illustrates the different contributions to the emission spectrum in the visible and near infrared regions. Deducting the soot continuum contribution to the measured emission intensity of CH radicals (see zoom of figure 1), the CH+CO relative intensity, φ_{CO+CH}, is defined as the percentage of the total emission $\mathbf{I_m}$, due to CH radicals and CO continuum. The soot contribution was estimated by means of the usual two wavelengths method

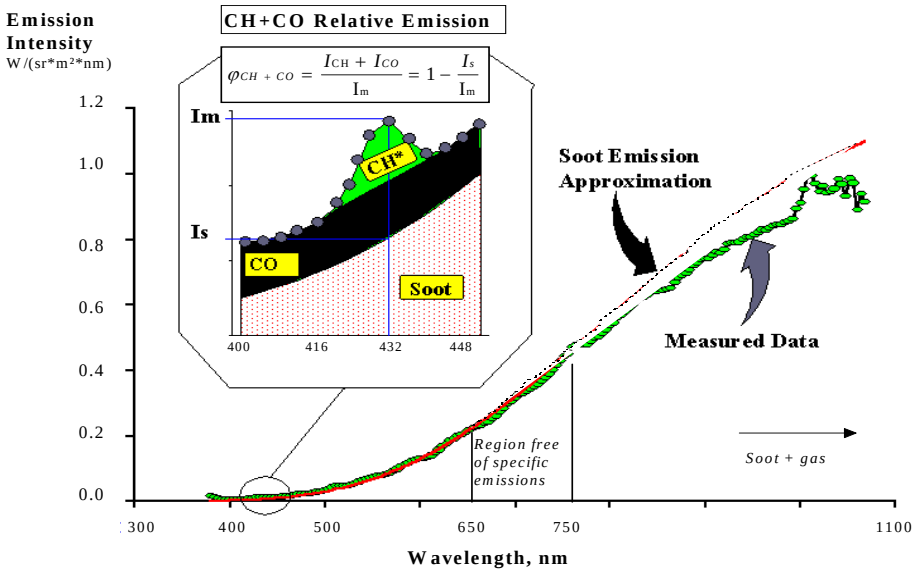

Figure 1: *Typical spectrum of a confined fuel oil flame*

[20,21,22] in a region of the spectrum, free of specific emissions [14]. In this study, 648 and 752 nm were used for that purpose.

In the range of air excess where the domestic boilers usually work, the NO emission decreases with the air excess [20,23]. On the other hand, the boiler thermal efficiency increases when the air excess is decreased. Thus, the objective of a combustion control system is to achieve a minimum air excess at which the CO and soot emission levels are still negligible.

The main advantage of the φ_{CO+CH} function is the superposition of two opposed effects: the CH radicals, precursors of the fuel and prompt NO [20,24], and the CO emissions. Previous results [3], obtained the boiler being working at high firing rate, have shown that φ_{CO+CH} decreases with the air excess to a minimum value, which coincides with a sudden CO increase. The optimal boiler performance is well defined by the minimum of φ_{CO+CH}. However, in the case of very sooty flames, as those produced when the boiler operates at low

firing rate [20], the soot emission can reduce the effect of the CO increase. That is why to establish a general control strategy, additional criteria are needed.

3. DESCRIPTION OF THE TEST BENCH

The experimental apparatus, sketched in figure 2, consists in three basic components: the plant, represented by the ensemble burner-boiler, the spectrometer and the controller itself.

For a given load, this latter is aimed at an optimisation of the burner adjustment which leads to a maximal boiler thermal efficiency, minimal pollutants emission and a stable flame. Furthermore, an adaptability to external conditions as air and fuel properties is required.

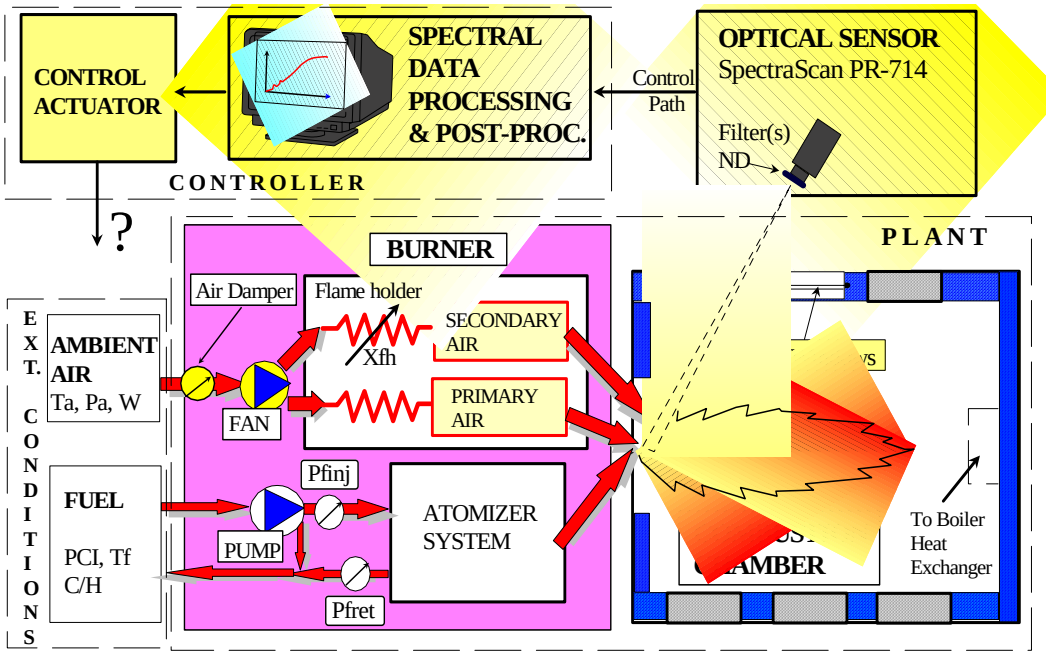

Figure 2: *The Test Bench and the control variables*

3.1 The burner-boiler combination

The fuel oil boiler used in this investigation has an nominal power of 370 kW and was equipped with a two firing rates burner. It is a commercial one, except the fact that for the flame spectrum recording, an optical access is available in the combustion chamber by means of two quartz windows of about 0.3*0.5 m² each.

Two typical burners (available on the market) were previously tested on that boiler in order to acquire background on the influence of different operating conditions. For our control application, a burner equipped with a spill-return atomizer was used for its flexibility to vary the flame holder position [25]. In addition, the burner power may be changed without a degradation of the fuel atomization quality, since the fuel injection pressure remains quite constant.

For a given power, the adjustment of the air circuit of a burner consists usually in adjusting the air damper angle and the flame holder positions. In practice, one finds on the market,

burners whose flame holder is either fixed or whose position varies with the burner power [23].

Figure 3 shows characteristic curves of the air circuit adjustment for the tested burner. On can observe that the same air mass flow rate, and therefore, the same overall air excess for a given fuel mass flow rate may be obtained with different flame holder and damper positions. In the

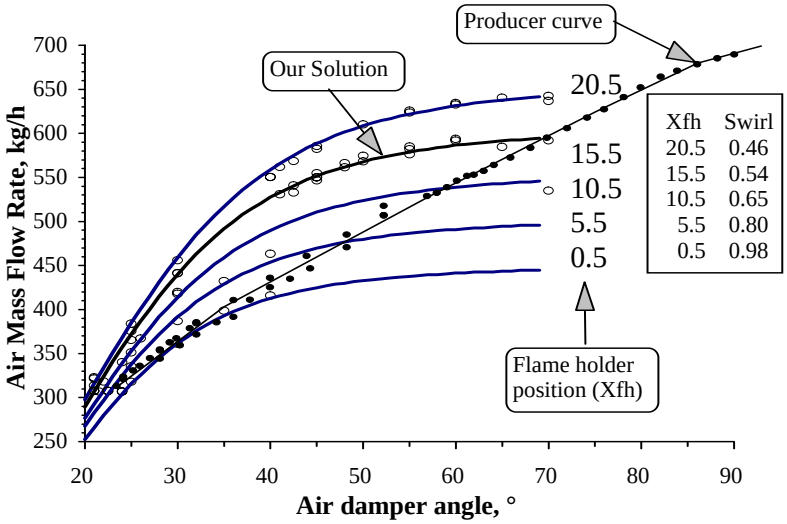

Figure 3: *Characteristic curves of the air circuit*

following text, the flame holder has been set to a fixed position X_{fh}=15.5, which gives a swirl number equal to about 0.54.

3.2 The Spectrum recorder

A spectrometer, operating in the visible and near infrared regions of the spectrum (from 380 to 1100 nm), provides the optical feedback from the flame. That device, described by Ngendakumana et al. [14], has been used in a first stage for an identification of the flame spectrum. Despite its poor intrinsic spatial resolution compared to laser-based techniques, it was chosen for its cheapness and adaptability to the available optical access [15].

The spectrometer focused the main reaction zone of the flame from a distance of 3.5 m to the burner exit with an angle of 40° from the flame axis. The measuring spot is thus a rectangle of about 92*30 mm². The viewing angle and the focusing distance were chosen in order: a) to obtain a representative spot of the flame front where the radicals emissions signal is the strongest, and b) to prevent excessive heating of the optical head by incoming radiation.

The accuracy of the spectral data is expected to be equal to 0.5% of the maximum peak response, which is located in the near infrared region (see figure 1). However, the utilisation of a neutral density filter (ND8X) help to attenuate the radiation in that region of the spectrum and thus to improve the accuracy. For high luminous flames, a filter is also needed to prevent overloading of the detector. Care has also to be taken to avoid soot deposition on the boiler quartz windows, which occurs when the air excess is reduced below a critical value. Indeed, in that case, the quartz

transmission coefficient is altered. Thus for a safe operation of the control system, this later must detect in time that critical value of the air excess.

3.3 Data Processing and Control Actuation

3.3.1 *Spectral data recording and pre-processing*

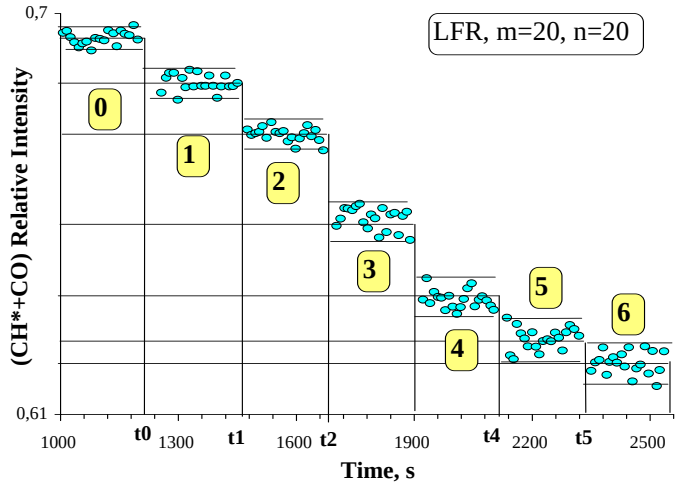

Figure 4: *Example of the sampling procedure*

The on-line acquisition of the flame spectrum is carried out by an PC 486 connected by an interface card to the spectrometer. Figure 4 illustrates the sampling procedure used in the processing stage, where each flame state (k=0,..,6), associated to at a given specified air damper position γ, is evaluated statistically by a series of **m** measures, each measure being obtained through **n** integrating cycles. The time of each integrating cycle is optimised by an automatic adaptive function integrated in the device software. Usual measurement time varies between 10 to 6000 μs according to the light intensity. A high number of the integrating cycles results in a decrease of the signal noise, but also in an increase of the measurement period.

3.3.2 *The controller system*

The implementation of the control actuation system on the air damper has been achieved by modifications in the original electric circuit of the burner whose normal logic operation was simulated by a microprocessor. Figure 5 sketches the different components of the actual control system.

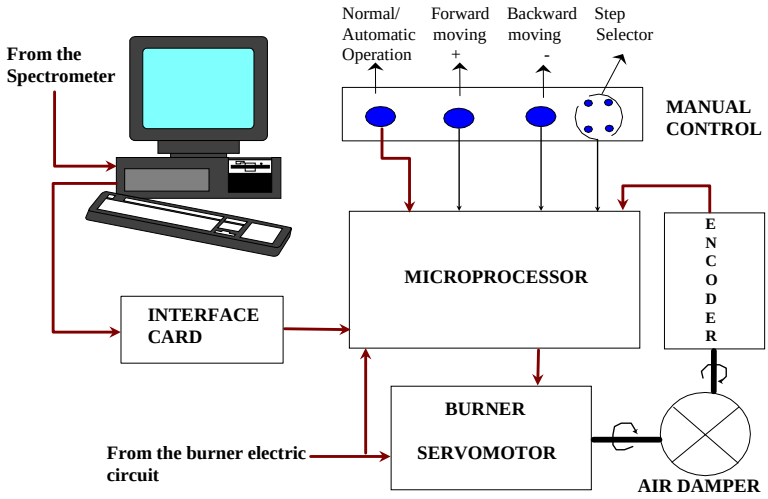

Figure 5: *The controller system*

The air damper angle was recorded by means of a rotary incremental encoder installed on the rotation axis of the air damper and whose resolution is 1024 pulses per revolution. Since it gives not only the position for rotating but also the direction of rotation, a fine processing of its output signal allows one to get a resolution of 0.1°. It is mainly the performance of the burner servomotor which limits the air damper position to 0.35° in order to keep a stable control loop.

The air damper angle can be controlled: a) automatically from a main program (the orders are sent to the microprocessor through an interface card and then to the burner servomotor); b) by using the original burner control (normal operation); and c) manually (two bottoms are available for the forward and backward moving and a four positions selector is used to set the damper angle step).

4. OPERATING CONDITIONS FOR AN OPTIMAL CONTROL

4.1 The burner adjustment and the boiler performance

4.1.1 *The boiler thermal efficiency*

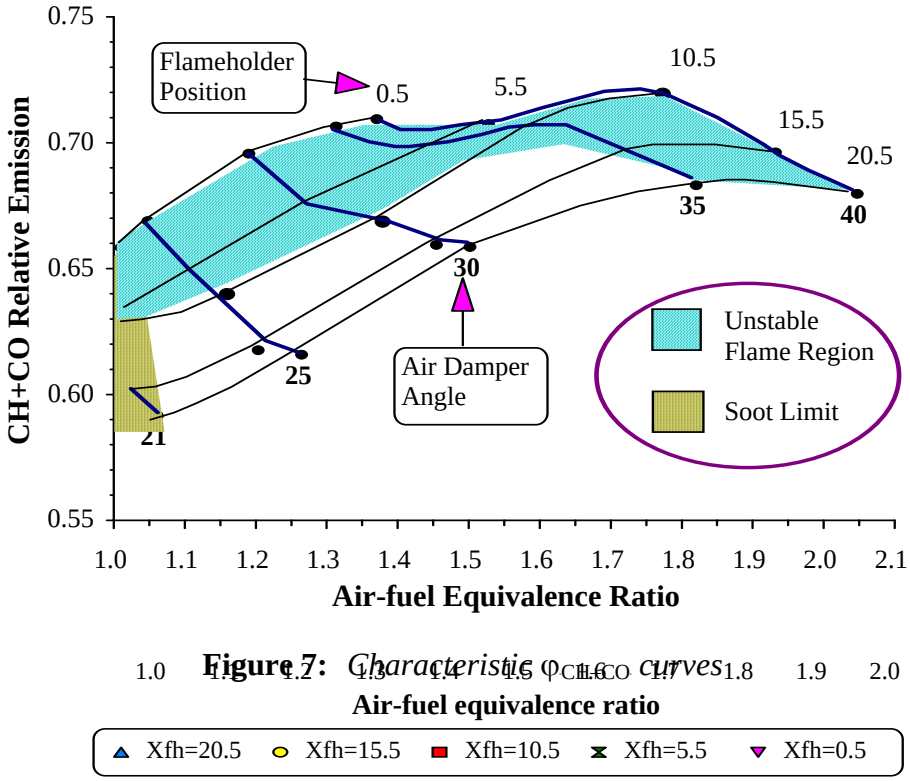

Figure 7: *Characteristic φ_{CH+CO} curves*

Figure 6: *Influence of the air circuit adjustment on the thermal efficiency of the boiler*

Figure 6 gives for a fixed power of the burner, the evolution of the thermal boiler efficiency against the air-fuel equivalence ratio for different positions X_{fh} of the flame holder. It shows clearly the well know dependency of the boiler thermal efficiency on the global air excess [26]. The adjustment of the flame holder position do not have any significant effect on the global thermal efficiency.

4.1.2 *The flame stability and the soot limit*

Figure 7 gives the characteristic curves of the φ_{CH+CO} variable for different flame holder and air damper positions. It shows the main operating regions of the flame. In the region of low air excess, a decrease of the flame holder position allows one to reach lower air excess values without producing soot at the chimney. But for flame holder positions $X_{fh} \leq 10.5$, the flame becomes unstable. Those positions agree with swirl numbers higher than a critical value of 0.6, over which large re-circulation zones and high levels of turbulence are generated [27].

Figure 8 shows the evolutions of the gas temperature T_{gCC} (measured at the combustion chamber exhaust) and the CH emission intensity if the flame holder position is decreased progressively, the air damper angle being fixed at $\gamma = 23°$. From that figure, it appears that the flame start to become unstable at $X_{fh}=10.5$. Notice also the effect of soot on the measured CH emission intensity at $X_{fh}=5.5$. One observes a CH emission decrease due to a decrease of the window transmission coefficient by soot deposition. Thus, the position $X_{fh}=15.5$ appears to be an optimal one for our control purpose.

4.2 The system response to external influences

The fuel temperature and type as well as the combustion air temperature have a non negligible influence on the fuel-air mixing process and thus on the pollutants emission [25]. The ability of the flame spectrum to detect the main disturbances is discussed here after.

4.2.1 *Influence of the air temperature*

Figure 9 gives the evolutions of the air temperatures at the burner inlet ($\mathbf{T_{ac}}$) and within the burner head ($\mathbf{T_a}^*$) for two tests carried out in similar conditions. Test A (constant ambient temperature) shows that the burner fan produces an additional heating which increases when the air mass flow rate, $\mathbf{m_a}$, decreases. From those results, the temperature $\mathbf{T_a}^*$ can be estimated by:

$$T_a^* = T_{ac} + \frac{0.662}{\dot{m}_a}$$

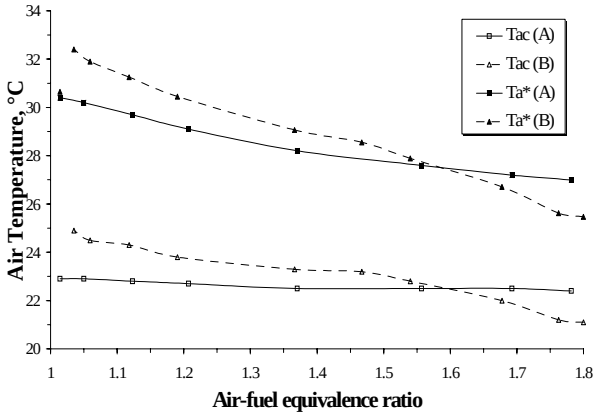

Figure 9: *Evolutions of air temperatures for A and B tests.*

The influence of the air temperature on the NO emissions is observed on figure 10. That effect is also well detected by the φ_{CH+CO} signal (figure 11). The increase of NO with the air temperature may be explained either by the convective effect of the primary air (which is in direct contact with the fuel jet) on the evaporation time and thus on the heat release profile, or by the increase of the flame temperature.

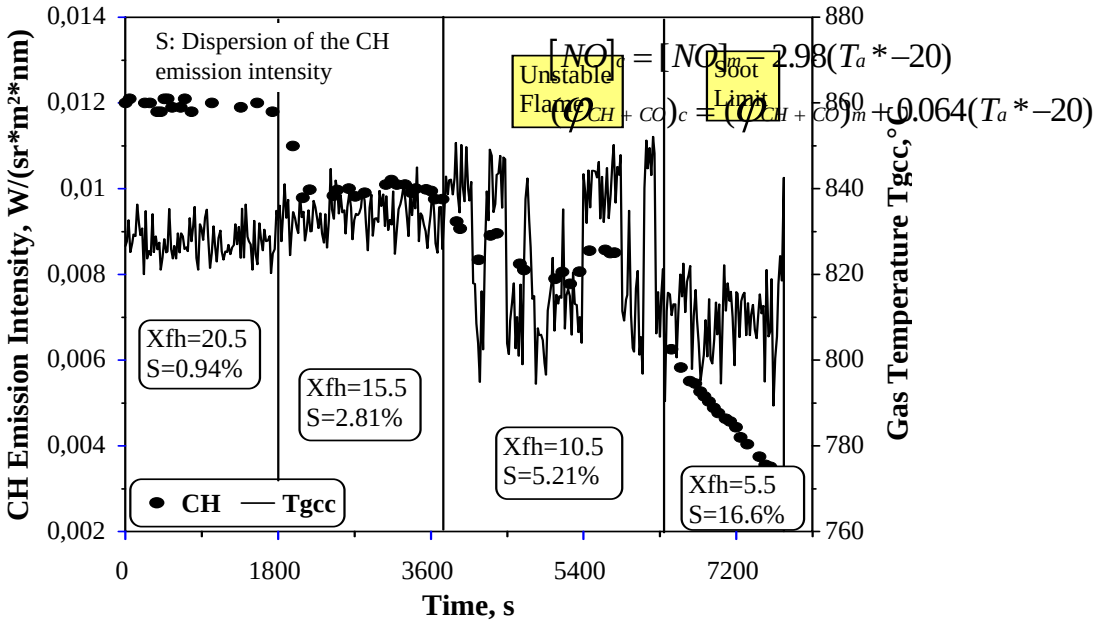

$$[NO]_c = [NO]_m - 2.98(T_a^* - 20)$$

$$(\varphi_{CH+CO})_c = (\varphi_{CH+CO})_m + 0.064(T_a^* - 20)$$

Figure 8: *Influence of the air swirl on the flame stability*

The influence of the air temperature on the NO emission and the flame spectrum (φ_{CH+CO} variable) may be easily taken into account as illustrated on figures 10 and 11. Considering a standard condition of 20°C, the corrected values are given by:

where the subscripts 'c' and 'm' stand for corrected and measured values respectively

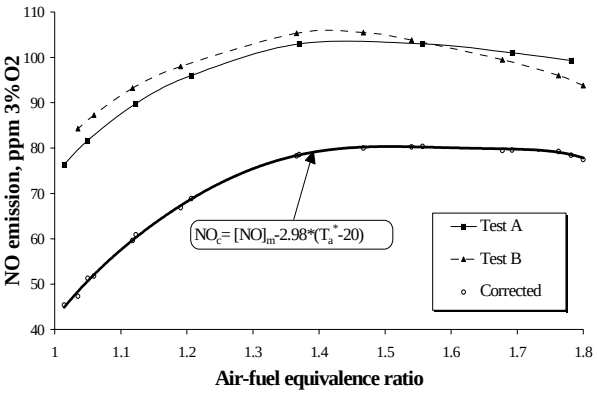

Figure 10: *Influence of air temperature on the NO emission*

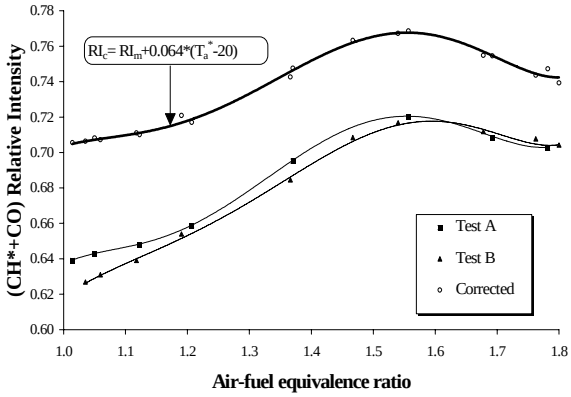

Figure 11: *Influence of air temperature on the flame spectrum.*

4.2.2 *The influence of the transient regime and the fuel temperature*

Figure 12 shows the evolution of φ_{CH+CO} starting when burner is ON. During the first 2.5 hours, where the fuel temperature was maintained constant at 20°C approximately, one observes that it takes about 30 minutes to get a stabilised flame spectrum. That stabilisation period, which is also observed on the evolutions of CO and NO emissions (figure 13), is attributable mainly to the effect of the burner head warming up.

In the second part of the test, the importance of the fuel temperature on the flame spectrum and on the NO emission is displayed. The φ_{CH+CO} variable follows well the NO increase with the fuel temperature. An increase of the fuel temperature results in a decrease of the fuel viscosity and thus the mean droplet diameter in the fuel spray. The fuel-air mixing quality being improved, the soot emission is thus decreased [25] while the NO emission is increased [7].

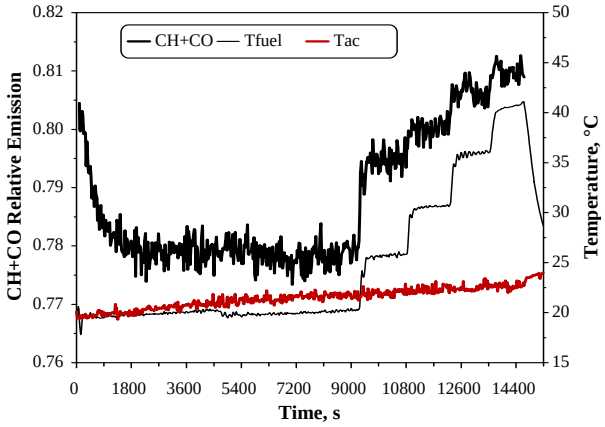

Figure 12: *Influence of the transient regime and the fuel temperature on the flame spectrum*

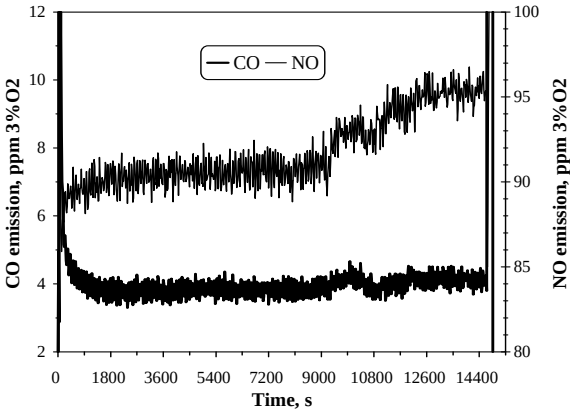

Figure 13: *Influence of the transient regime and the fuel temperature on the pollutants emission*

4.2.3 *The fuel chemistry*

The flame spectra recorded with fuels from different deliveries are very different. This is shown in figure 14, which gives the evolution of φ_{CH+CO} , the burner being fed by fuel A, B and A successively. Notice also that when the burner is fed again with fuel A, one recovers the initial spectrum signal.

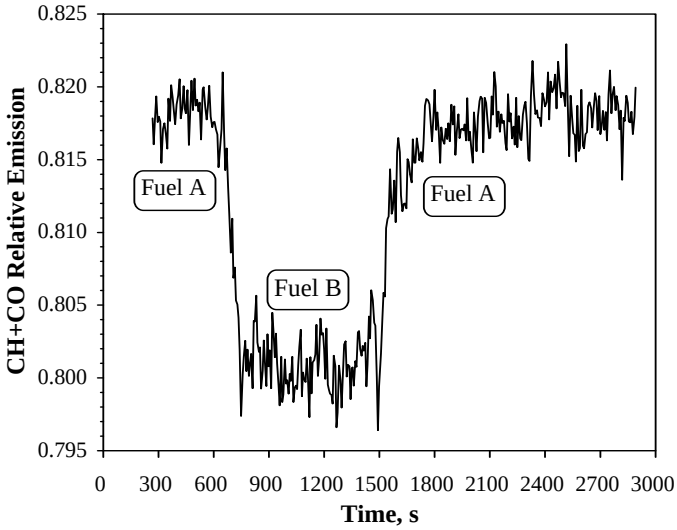

Figure 14: *Effects of the fuel on the flame spectrum*

In order to investigate the role played by the fuel on the pollutants emission and the optimal burner adjustment, tests have been carried out with two fuels : A and B. For the two kinds of tests, care has been taken to keep the same working conditions for the burner-boiler combination. A comparison of the results thus obtained is given in figures 15 and 16 for the NO emissions and the flame spectra respectively.

About the NO emission, a difference of about 15 ppm is observed between the two fuels (figure 15) and is attributed to the fuel NO formation mechanism. Indeed, from a study on the nitrogen content in different light fuel oils available on the belgian market [28] and assuming a 100% fuel nitrogen conversion to NO [29], the contribution of fuel NO to the overall NO may vary from 13 to 30 ppm [30].

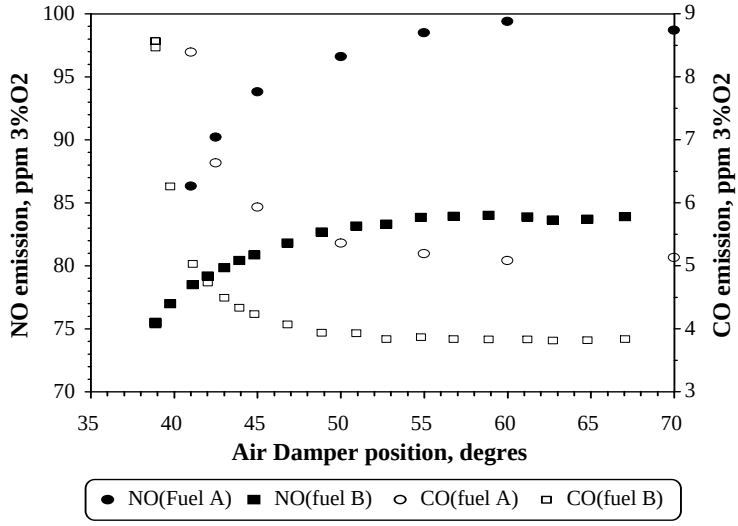

Figure 15: *NO and CO emissions*

In addition to the higher NO emission level reached with fuel A, soot radiation levels are 3 times greater than those obtained with fuel B. Those differences may be explained by possible changes in the fuel composition (C/H ratio) from the oil-refinery.

Finally, figure 16 shows how the φ_{CH+CO} variable is able to take into account the changes in the fuel composition. Given the lower soot level obtained with fuel B, the optimum damper angle is found ≈2.5° below that corresponding to fuel A. This is equivalent to a higher reduction of air excess and NO emission.

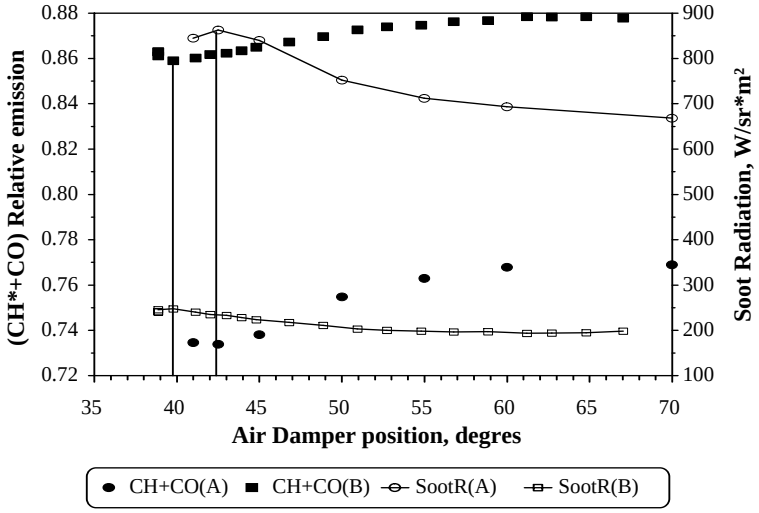

Figure 16: *Control variables evolution*

CONTROL STRATEGY AND PRELIMINARY RESULTS

5.1 The Combustion Control Strategy

A general combustion control strategy must be able to meet the power load requirements. Thus, an adaptation is desired for different burner firing rates. In a first attempt, two extreme firing rates (the low firing rate HFR and the high firing rate HFR), corresponding to a burner power equal to 246 and 416 kW respectively, have been considered.

The approach is explained in terms of a statistical analysis of each data sample associated to a specified position of the air damper (figure 4). The idea consists in a gradual reduction of the air damper angle until a critical value characterised by excessive CO and/or soot emissions is reached. Recall that a reduction of the air excess is advantageous from the thermal performance of the boiler and NO production. For example, a reduction from 40% to 5% in figures 6 and 10 is equivalent to an increase of the boiler efficiency and a reduction of NO emission of about 2% and 37.5% respectively.

According the results shown in figure 16, there exist at least two ways to go toward the optimal condition: a minimisation of the j_{CH+CO} function or a maximisation of the soot radiation (R_{soot}).

Figure 17 shows the flow diagram of the control strategy used. The on-line procedure considers three basic tests that guides the air damper excursion to an optimal position γ^*.

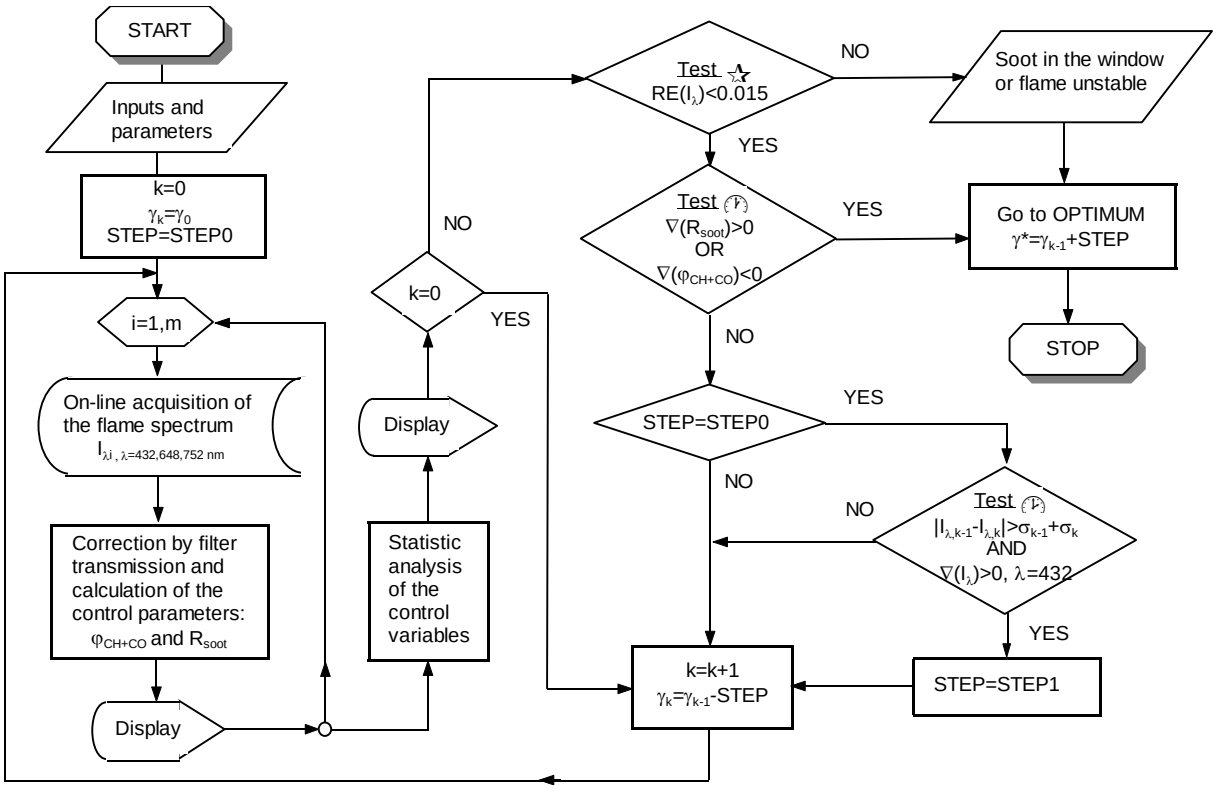

Figure 17: *Flow diagram of the control strategy*

5.1.1 *The imposed conditions*

Before starting the optimisation procedure, a certain number of parameters have to be to fixed: the initial air damper position γ_0 , the angle step for the first iteration STEP0, the accuracy of the spectrum data, the fuel and combustion air temperatures.

The initial position of the air damper was chosen as the inflexion point of the φ_{CH+CO} function (fitted by a polynomial of third degree of air damper angle γ). Applying this criterion to the previous results, one found values of γ_0 equal to 28° and 49° for the low and high firing rates respectively .

Two angle steps are applied in the optimisation process. A first step of 2° is used as initial condition. The change to a smaller step of 1° is made when the measured CH emission (at 432 nm) begins to decrease. Recall that the CH emission begins to decrease with the air excess before soot radiation [20].

At each air damper position, 10 measures of the flame spectrum have been performed, and 20 integration cycles have been adopted to improve the measurement accuracy.

Concerning the external conditions, the fuel temperature was controlled and fixed to about 20°C. The combustion air was also conditioned in order to avoid its temperature increase due to the heat losses through the boiler windows.

The optimisation procedure has been started the system being in steady-state regime, say about 30 minutes after the burner is ON.

5.1.2 *The sample dispersion and the flame stability (Test 1)*

A first one test analyses the relative errors affecting the measured CH radicals (432 nm) and soot (648 nm) emission intensities. According to previous tests, using m=10 measures and n=20 integrating cycles, the relative error RI(I) must be smaller than 1.5% for an acceptable functioning. For each k^{th} sampling data, that condition is equivalent to:

$$RE_k\left(I_\lambda\right) \equiv \left(\frac{\sigma_{I_\lambda}}{\bar{I}_\lambda}\right)_k < 0.015 \qquad (1)$$

where $\bar{I}_\lambda$ and σ_{I_λ} are the averaged m-values of the emission intensity at the wavelength λ and its standard deviation respectively.

In general, that condition is fulfilled, but it is not the case if soot deposition on the windows and flame instability occur.

5.1.3 *Research of the optimal condition (Tests 2)*

A second one test consist in an analysis of the gradient ∇(X) of a control function X, which is defined by:

$$\nabla_k(X) = \frac{\overline{X}_{k-1} - \overline{X}_k}{\gamma_{k-1} - \gamma_k} \tag{2}$$

where $\overline{X}_k$ is the mean value of the variable X and γ_k is the air damper angle at the k^{th} iteration.

∇(X) is useful in the search and identification of the optimal condition. Of course, if the sign of the φ_{CH+CO} function is negative or if the sign of the soot radiation R_{soot} is positive, then, the optimal position will correspond to the previous one ($\gamma^*=\gamma_{k-1}$).

5.1.4 *Approximation to the optimum with a fine tune (test 3)*

The last test anticipates the time when the system reaches the optimal condition in order to approach it with a fine tune. This time is identified by means of two conditions imposed to the CH emission intensity (at 432 nm):

a) The first one compares the averaged intensities for the k and k-1 positions with its standard deviation by means of the equation (3). That condition checks if those two measures are statistically distinct or not.

$$\left|\bar{I}_{432,k} - \bar{I}_{432,k-1}\right| > \left(\sigma_{I_{432}}\right)_{k-1} + \left(\sigma_{I_{432}}\right)_k \tag{3}$$

b) A second one is imposed on the gradient of the CH emission intensity in the next terms.

$$\nabla_k(I_{432}) \equiv \frac{\bar{I}_{432,k-1} - \bar{I}_{432,k}}{\gamma_{k-1} - \gamma_k} > 0 \tag{4}$$

Therefore, if the conditions given by equations (3) and (4) are satisfied, the system send the order to approach with a low step STEP1=STEP0/2. This condition helps among others to prevent soot deposition on the boiler quartz windows.

5.2 Preliminary Results

5.2.1 *Tests in high firing rate*

Figures 18 and 19 show for the high firing rate, the evolutions of the control variables and pollutants emission, respectively. For this operating condition, the critical positions associated to both R_{soot} and j_{CH+CO} variables coincide with the optimum below which CO starts to increase strongly ($\gamma^*=\gamma_5$). In this case, the controller receives the stop order at the 6th iteration since the gradient of the control variables does not satisfy the condition imposed by test 2.

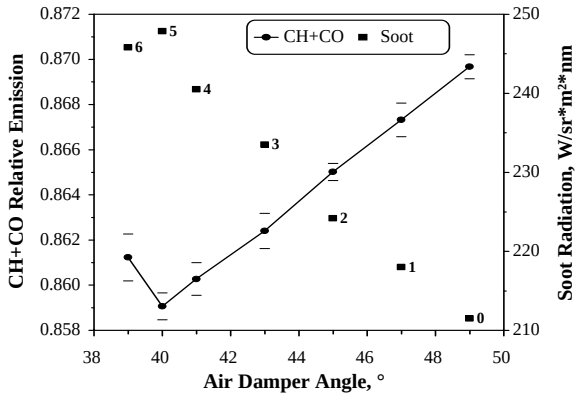

Figure 18: *Spectrum data at HFR*

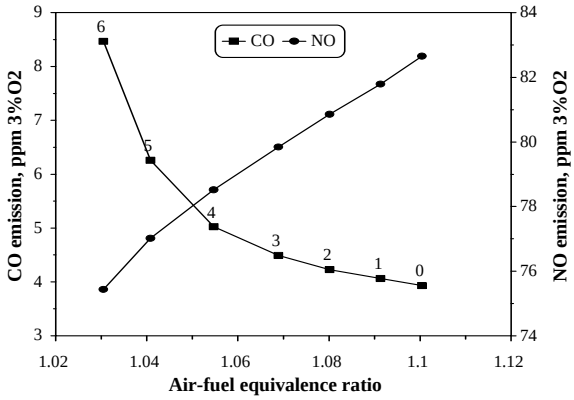

Figure 19: *CO and NO emission at HFR*

Figure 20 which gives the evolutions of the measured emission intensities at 432 nm and 648 nm, shows that the CH radicals emission start to decrease just after the 4th iteration. At that time event (test 3), an order is given by the controller to change the angle step for the next iteration. Notice also that the maximum of the soot emission (at 648 nm) coincides with that of the soot radiation (figure 18).

Figure 21 shows that the relative error associated with the j_{CH+CO} variable is always negligible (less than 0.2%). On the other hand, despite a slight increase of the scattering of individual emission intensities, that scattering is less than the measurements accuracy (1.5%).

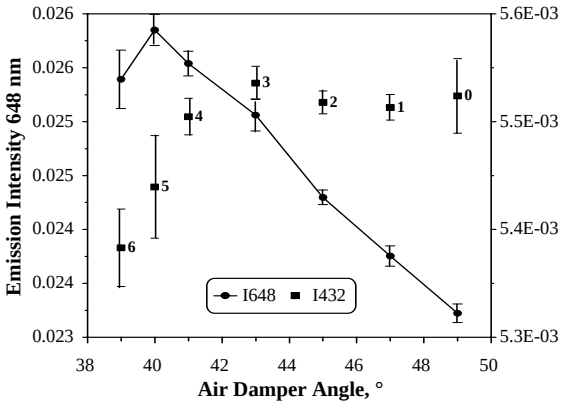

Figure 20: *Evolution of soot and CH emissions at HFR*

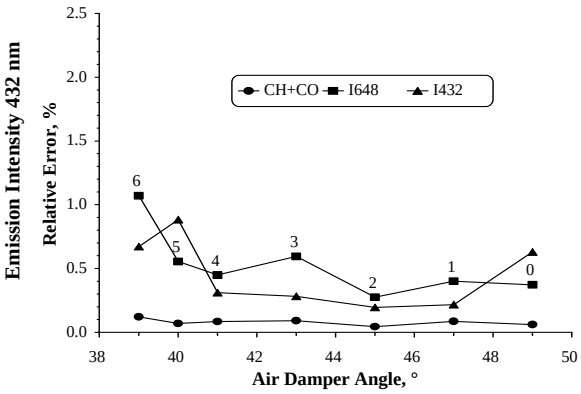

Figure21: *Spectrum data scattering at HFR*

5.2.2 *Tests in low firing rate*

The low firing rate operating condition is characterised by a flame of high luminosity. A comparison between figures 18 and 22 shows that the soot radiation level in LFR condition is 5 times higher than in HFR condition. With a spill-return atomizer, the fuel injection pressure is quite constant at different burner power. However, the lower air velocities associated to the LFR condition reduce the fuel-air mixing strength and thus fuel rich zones in the flame are favourable for soot formation.

In that case, the j_{CH+CO} curve (figure 22) do not go through a minimum as for the HFR condition. A local stabilisation is however observed at the 5th iteration, which coincides with the point where CO start to increase (figure 23). Soot radiation is maximum at the limit of operation (k=6) after which, CO increases excessively and soot is observed in the flue gas at the chimney (Bacharach index higher than 1). About NO emission, figure 23 shows a reduction close to 16% when the air damper angle is reduced from the initial condition γ_0 to the optimum $\gamma^*=\gamma_6$.

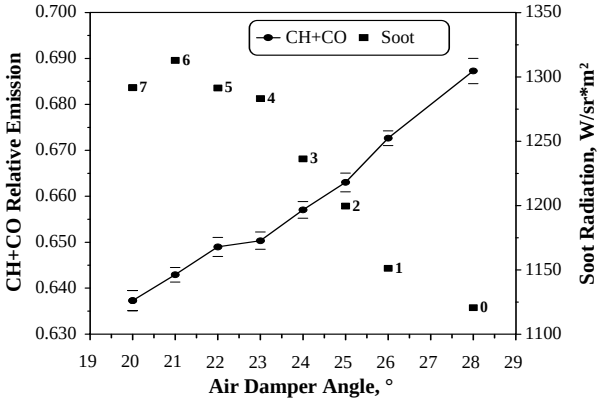

Figure 22: *Spectrum data at LFR*

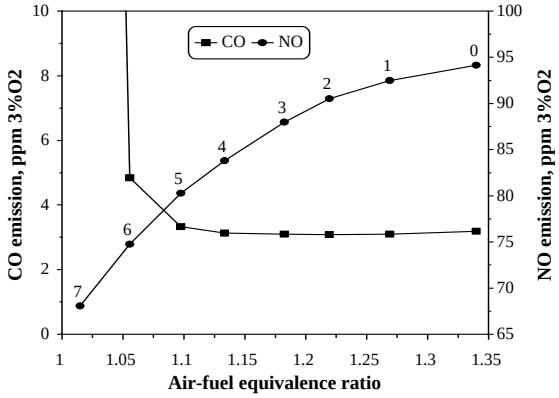

Figure 23: *CO and NO emissions at LFR*

Figure 24 shows that in LFR operating condition, the CH radicals emission intensity decreases continuously when the air excess is decreased, contrary to what happens in HFR condition (figure 20).

Finally, the non coincidence of the maximum soot emission measured at 648 nm with the calculated maximum soot radiation indicates a possible reduction of the quartz transmission coefficient due to soot deposition on the window. This is confirmed by the emission scattering (figure 25) which increases in the two last iterations, reaching values higher than the critical limit given in test 1 (1.5%).

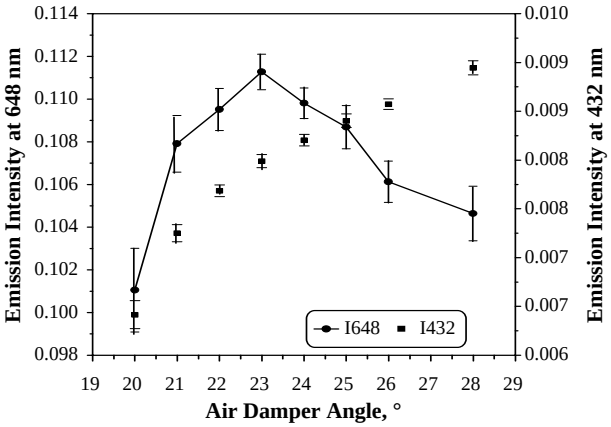

Figure 24: *Evolutions of soot and CH emissions at LFR*

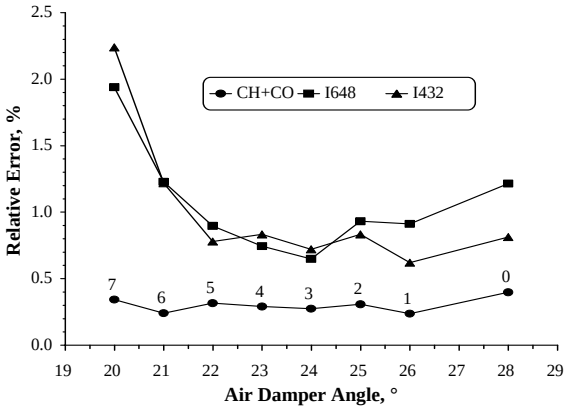

Figure 25: *Spectrum data scattering at LFR*

CONCLUSIONS

The feasibility of an automatic combustion control, relying entirely upon CH radicals and soot emissions recorded in the main reacting region of the flame, has been demonstrated in a fuel oil boiler. The control system meet simultaneously energetic and environmental requirements for an optimal boiler performance.

For a given burner power, the control strategy consists in achieving the minimum air excess that assures an operation without excessive CO and soot in the flue gases at the chimney. Characterisation tests of the system have shown that the flame holder may be fixed at a position corresponding to a swirl number equal to about 0.54 and only the air damper has to be varied.

The combination of the CH radicals and soot emissions provides the necessary criteria for the development of an optimal strategy. Soot radiation appears as the best tracer for an optimal operating condition, whereas CH radicals give additional criterion on the flame stability and help to guide the excursion to the optimal condition. Pollutants emissions (NO, CO and soot) are gathered implicitly in a new spectral parameter, the CH+CO relative intensity, which appears as a good tracer of combustion. Disturbances produced by external conditions are well detected.

The control strategy proposed is able to take into account different inputs conditions (the burner power and the fuel composition) which can have a significant impact on pollutants emission. Changes in fuel composition have been identified as the most important cause of observed differences on NO emission levels. Concerning the burner power, the high soot emission level observed in low firing rate condition is due to the lower air velocities associated to that condition.

ACKNOWLEDGEMENTS

This work was financially supported by the Walloon Ministry for Technology and Energy (Belgium) under the research project "Investigation of Combustion in Oil Burner Flames" in the frame of IEA-Combustion activities.

The authors wish also to acknowledge the VIESSMANN, WEISHAUPT and ABIG manufacturers, and are grateful to Mr R. Labenda for his technical assistance in the different tests and to Mr P. Ruwet for his contribution in the realisation and programming of the actuator control system.

NOMENCLATURE

I_l	Spectral emission intensity, W/(sr*m²*nm)
l	Wavelength, nm
φ_{CH+CO}	CH+CO Relative emission intensity
R_{soot}	Soot radiation, W/(sr*m²*nm)
RE(X)	Relative error associated to the variable X
∇(X)	Gradient of a variable X
X_{fh}	Relative position of the flame holder, mm
γ	Air Damper Angle, °
T	temperature, K (°C)
$\dot{m}$	Mass flow rate, kg/s
STEP	The angle step for one iteration
γ_0	The initial air damper angle
γ*	The optimal air damper angle
k	The iteration number
m	Number of measurement for each iteration
n	number of integrating cycles of one measure

REFERENCES

[1] ATIC, "Les émissions polluantes des chaudières: Unités et valeurs limites", Chaleur et Climats 623/91/06.

[2] GARG A., Chemical Engineering Progress, p. 46, January, 1994.

[3] NGENDAKUMANA Ph. and FARIAS O., "Automatic Control of Combustion in Fuel Oil Boilers", IEA Combustion Agreement Task Leaders Meeting, Cranfield University, United Kingdom, august 6-9, 1996.

[4] ALLEN M., BUTLER C., JOHNSON S., LO E, and RUSSO F, Combustion and Flame 94:205-214, 1993.

[5] LEVYNSKY H.B., "Between Research and Development: Using Laser Diagnostics and Numerical Models to Evaluate Practical, Natural-Gas-Fired Burners", EUROTHERM Seminar N°35, Leuven (Belgium), may 26-27, 1994.

[6] FAETH G. and KÖYLÜ U., "Soot Morphology and Optical Properties in Nonpremixed turbulent flame environments", 2nd International Conference on Combustion Technologies for a Clean Environment", Lisbon (Portugal), 1993.

[7] BOWMAN C.T, 14th Symposium (International) on Combustion, p.729, The Combustion Institute, 1992.

[8] GAYDON A.G. and WOLFHARD H.G., "Flames : their structure, radiation and temperature", Chapman and Hall Ltd, 1970.

[9] ALLEN M.G. and HANSON R.K., 21st Symposium (International) on Combustion, p. 1755, The Combustion Institute, 1986.

[10] SCHULER F., RAMPP F., MARTIN J., and WOLFRUM J, Combustion and Flame 99:431-439, 1994.

[11] BOWMAN C.T., PADMANABHAN K.T. and POWELL J.D., Combustion and Flame 100:101-110, 1995.

[12] WOHL K., CHILD E.T., and KUSHIDA R., 7th Symposium (International) on Combustion, p. 215, The Combustion Institute, 1958.

[13] CHOU T. and PATTERSON D.J., Combustion and Flame, 101:45-57, 1995.

[14] NGENDAKUMANA Ph., ZUO B. and WINANDY E., "A spectroscopic study of flames for a pollutant formation regulation in a real oil boiler", 2nd International Conference on Combustion Technologies for a Clean Environment. Lisbon (Portugal), 1993.

[15] NGENDAKUMANA Ph. and FARIAS, "The influence of the operating conditions of a fuel oil boiler on the flame spectrum". Eurotherm seminar N° 35. Leuven (Belgium), 1994.

[16] TICHY F., TAKAHARA T., BJORGE T. and MAGNUSSEN B.F., "Experimental investigation on turbulent acetylene flames", IEA-Energy Conservation and Emissions Reduction in Combustion, Liège (Belgium), may 26-27, 1995.

[17] CHECKEL M. and THOMAS A., Combustion and Flame 96:351-370, 1994.

[18] BIELERT U., KLUG M. and ADOMEIT G., Combustion and Flame 106:11-28, 1996.

[19] MIZUTANI Y., NAKABE K., MATSUMOTO Y., SAEKIT and MATSUI T., JSME International Journal, Series II, Vol. 32, N°3, 1989.

[20] FARIAS O. and NGENDAKUMANA Ph, Bull. Soc. Chim. Bel. Vol. 105, n° 9, 1996.

[21] CHOI M.Y., HAMINS A., MULHOLAND G.W., and KASHIWAGI, Combustion and Flame 99:174-186, 1994.

[22] COPPALLE A. and JOXEUX D., Combustion and Flame 96:275-285, 1994.

[23] NGENDAKUMANA Ph.,"Domestic fuel oil burner-boiler matching: Laboratory Test Results" 1st European Conference on Small Burner Technology and Heating Equipment", 1st European Conference on Small Burner Technology and Heating Equipment, Zurich (Switzerland), 1996.

[24] HEARD D.E., JEFRIES J.B., SMITH G.P and CROSLEY D.R., Combustion and Flame 88:137-148, 1992.

[25] FARIAS O. and NGENDAKUMANA Ph., "Influence of the Fuel-Air Mixing on the Flame Spectrum and Pollutant Emissions of a Fuel Oil Boiler", Internal report, Lab. of Thermodynamics, University of Liège (Belgium), February, 1997.
[26] LEBRUN J. and NGENDAKUMANA Ph., "Environmental nuisance of fuel oil burners at different regimes", Paper presented at the "Building Design Technology and Occupant well-being in Temperate Climates", Brussels (Belgium), 1993.
[27] GUPTA A., BEER J. and SWITHENBANK J., 16th Symposium (International) on Combustion, p. 79, The Combustion Institute, 1976.
[28] DE RUYCK J. and DISTELMANS M., "Comparative study on emissions from gas fired and oil fired residential boilers", 2nd International Conference on Combustion Technologies for a Clean Environment, p. 27.1-1, Lisbon (Portugal), 1993.
[29] TANG S., CHURCHILL S. and LIOR N., 18th Symposium (International) on Combustion, p. 73, The Combustion Institute, 1980.
[30] WINANDY E., "Contribution à l'étude de la Formation des NOx dans les Chaudières alimentées au Fuel Liquide", IRSIA activity report, Lab. of Thermodynamics, University of Liège (Belgium), 1994.